.Copy·
RM E54L31a

NACA

COPY 1

RESEARCH MEMORANDUM

FULL-SCALE, FREE-JET INVESTIGATION OF METHODS OF

IMPROVING OUTLET FLOW DISTRIBUTION IN A SIDE-

INLET SUPERSONIC DIFFUSER

By John M. Farley and Ferris L. Seashore

Lewis Flight Propulsion Laboratory
Cleveland, Ohio

NATIONAL ADVISORY COMMITTEE
FOR AERONAUTICS
WASHINGTON
March 28, 1955

NATIONAL ADVISORY COMMITTEE FOR AERONAUTICS

RESEARCH MEMORANDUM

FULL-SCALE, FREE-JET INVESTIGATION OF METHODS OF IMPROVING OUTLET

FLOW DISTRIBUTION IN A SIDE-INLET SUPERSONIC DIFFUSER

By John M. Farley and Ferris L. Seashore

SUMMARY

A full-scale, free-jet investigation has been conducted to determine the performance of a side-inlet supersonic diffuser, designed for a flight Mach number of 2.75. Several internal modifications, made to improve the diffuser-outlet flow uniformity, were evaluated. Among the modifications were a screen installed near the diffuser outlet, a four-stage vortex-generator configuration, and a 12-stage vortex-generator configuration. The effect of reducing the spans of the vortex generators in the 12-stage configuration was also determined.

Some improvement in flow distribution was obtained with all modifications investigated. The greatest improvement, however, was obtained with the 12-stage vortex-generator configuration. The longer-span modification of this configuration gave the greatest improvement in flow uniformity at intermediate pressure recoveries; at pressure recoveries above or below the intermediate range, the short-span modification gave the most uniform flow distribution. With the unmodified diffuser, flow separation occurred when the diffuser total-pressure recovery was as high as 0.60. With the reduced-span modification of the 12-stage vortex-generator configuration, separation did not occur until the total-pressure recovery was reduced to about 0.51.

INTRODUCTION

A full-scale, free-jet investigation has been conducted at the NACA Lewis laboratory in order to evaluate and improve the performance of a 48-inch-diameter ram-jet engine. The engine diffuser was a side-inlet type, designed for a flight Mach number of 2.75. The supersonic portion was, essentially, a 216° segment of a single-cone Ferri type diffuser. The internal portion of the diffuser was contoured to bend the air in toward the missile body and diffuse it to the 32-inch-diameter diffuser outlet.

Early in the investigation it was found that the flow at the diffuser outlet was poorly distributed and that separation occurred. As a result, combustor pressure losses were high and combustion occurred upstream of the flameholding elements. The diffuser manufacturer then initiated a scale-model investigation of methods of improving the diffuser flow distribution. As promising modifications were evolved from these scale tests, they were checked in the full-scale diffuser at the Lewis laboratory.

The data presented herein show the diffuser-outlet flow contours obtained in the full-scale investigation of the basic diffuser and the effect of several of the internal modifications made to improve flow uniformity. Among the modifications investigated were a screen located near the diffuser outlet and three arrangements of vortex generators in the diffuser duct. All data were obtained with a nominal free-stream Mach number of 2.75, with an angle of attack of 3°, and with the diffuser operating supercritically. The data presented were obtained with a nominal engine air flow of 80 pounds per second (the corresponding inlet total pressure was about 2600 lb/sq ft abs) and an inlet total temperature of 525° F. Data were obtained with both cold flow and the combustor operating.

APPARATUS

Basic Diffuser

A phantom sketch of the engine diffuser is presented in figure 1. Photographs of the diffuser are shown in figure 2, and the area variation through the diffuser in figure 3. The supersonic portion was, essentially, a 216° segment of a single-cone (22° half-angle) Ferri type diffuser, designed for a flight Mach number of 2.75. Boundary-layer bleed air was ducted below the main diffuser to the facility exhaust section.

Diffuser Modifications

Figure 4 is a photograph of the screen installed in the diffuser. The screen, which was constructed of 1/4-inch-diameter rods, was located about 21 inches upstream of the diffuser outlet and blocked 30 percent of the diffuser cross-section area.

The vortex-generator configurations are described in figure 5. Figure 6 is a photograph of a typical installation. Configuration VG-1 had three stages of vortex generators on the diffuser innerbody and one stage on the cowl. Configuration VG-2 had the original three stages and five

additional stages on the innerbody and four stages on the cowl. Configuration VG-2a was the same as VG-2 except that the spans of the vortex generators in the last nine stages were reduced 19 percent.

Combustor and Exhaust Nozzle

Transition from the 32-inch-diameter diffuser outlet to the 48-inch-diameter combustion chamber was accomplished with a 30° included-angle conical-diffuser section in which the flameholder and the fuel-injection system were mounted. The exhaust nozzle was equipped with a clamshell-type throttle so that diffuser pressure recovery could be varied when the combustor was not operating.

Installation

Figure 7 is a sketch of the engine installed in the free-jet facility. The facility supersonic nozzle was designed for a Mach number of 2.75. Air not captured by the engine diffuser was diffused to exhaust-section pressure by means of the jet diffuser. Reference 1 shows details of the free-jet facility and the supersonic-nozzle flow characteristics.

Instrumentation

Details of the instrumentation are shown in figures 7 and 8. Diffuser-inlet conditions were measured at the inlet to the supersonic nozzle (station 0), and the flow through the nozzle was assumed to be isentropic. The diffuser-outlet instrumentation station (station 3) was located about 28 inches upstream of the diffuser outlet. Instrumentation was installed at station 3' during the investigation of the screen configuration only.

PROCEDURE

Data were obtained over a range of pressure recovery from about 0.50 to critical. When fuel was not being burned (cold flow), diffuser pressure recovery was varied by means of the clamshell-type throttle mounted on the exhaust nozzle. When the combustor was operating, diffuser recovery was varied by changing the engine fuel-air ratio. When attempts were made to operate the diffuser in the subcritical region, the diffuser normal-shock wave interfered with the jet-diffuser action and the facility supersonic flow could not be maintained. Therefore, only supercritical data were obtained.

Range of Investigation

All data were obtained with the following inlet conditions:

Inlet Mach number, M_0 . . . . 2.75
Angle of attack, deg 3
Nominal engine air flow, lb/sec 80
Nominal inlet temperature, °F 525

Calculation

Symbols used are defined in appendix A. Methods of calculation are shown in appendix B.

RESULTS AND DISCUSSION

General Characteristics of Diffuser

Critical recovery. - The maximum diffuser pressure recovery recorded in the investigation of the unmodified diffuser was 0.629. Static instrumentation indicated that the diffuser was operating very close to the critical point when this recovery was measured. Because fully established supersonic flow could not be maintained in the test facility with the diffuser operating in the subcritical region, critical recovery values were very difficult to obtain. This facility limitation prevented any exact determination of the effect of the various vortex-generator installations on the diffuser critical recovery. However, pressure recoveries in the range from 0.625 to 0.635 were obtained when the vortex generators were installed. This indicated that the vortex generators had little, if any, effect on the diffuser critical recovery.

Diffuser supercritical mass-flow ratio. - The diffuser supercritical mass-flow ratio W/W_s was about 0.98. This value was calculated from an air-flow calibration of the engine and verified by calculations based on the position of the diffuser oblique-shock wave relative to the diffuser lip.

Effect of combustion on diffuser-outlet flow profiles. - Combustion had no significant effect on the diffuser-outlet flow profiles. Therefore, in general, only data obtained with cold-flow operation are presented herein. Hot-flow data were presented only when cold-flow data were not available for a given diffuser operating point.

3526

Effect of Diffuser Modifications on Flow Distribution

Performance of original diffuser configuration. - Diffuser-outlet
pressure recovery and Mach number contours, obtained with the original
(unmodified) diffuser configuration, are presented in figure 9. At all
values of pressure recovery, the flow crowded toward the left side
(viewed looking downstream) of the duct. Apparently the diffuser adverse
static-pressure gradient was too steep to allow the air to fully negotiate
the bends upstream (see fig. 2(b)). When the diffuser was operating with
an average pressure recovery of 0.629 (near critical), the local pressure
recovery varied from 0.555 to 0.703. The corresponding variation in Mach
number was from 0.15 to 0.62. When pressure recovery was decreased to
about 0.60, flow separation occurred at the 2 o'clock position. In the
high-velocity region, the Mach number increased with decreasing pressure
recovery until it became supersonic at values of pressure recovery be-
tween 0.58 and 0.59. When pressure recovery was further reduced, the
size of both the separated and supersonic regions increased. As a result
of these flow distortions, combustor pressure drops were very high and
combustion occurred in the separated region upstream of the flameholders.

Performance of screen configuration. - Small-scale tests, conducted
by the diffuser manufacturer, indicated that improvement in flow distri-
bution could be obtained by installing a screen at the diffuser outlet.
It was recognized that screen pressure drops would be high, but the im-
provement in flow distribution seemed sufficient to merit full-scale in-
vestigation, until more satisfactory methods of flow improvement could
be found in the small-scale apparatus.

Performance of the diffuser with a 30-percent-blockage screen located
near the diffuser outlet is shown in figure 10. Although the regular
diffuser-outlet instrumentation station (station 3) was located approxi-
mately 10 inches upstream of the screen, it might be expected that any
redistribution of the flow would be apparent in the readings at station 3.
The flow contours at station 3, however, do not show any significant im-
provement in uniformity (fig. 10(a)). At all values of pressure recovery,
the pressure-recovery contours show a greater difference between maximum
and minimum local recoveries when the screen was installed (figs. 9 and
10(a)). The Mach number contours show that, with high values of pressure
recovery (above 0.6), the peak Mach numbers were higher than and the low
Mach number regions were about the same as those obtained without the
screen. With lower values of pressure recovery (0.548 and 0.573), peak
Mach numbers were lower, but the separated regions were not improved by
the screen. It was also noted that the circumferential variations in wall
static pressure were greater when the screen was installed (i.e., static
pressure was lower in the low-velocity region and higher in the high-
velocity region). This greater variation was probably a result of in-
creased radial flow caused by the screen.

The distribution of pressure recovery behind the screen is shown in figure 10(b). In the low-velocity regions, local pressure recoveries are about the same as the corresponding values at station 3. In the high-velocity regions, however, large reductions in pressure occurred. It is not known if the separated regions, shown in the station 3 contours, persisted downstream of the screen because: (1) the static-pressure instrumentation downstream of the screen was not operative, and (2) the circumferential location of the minimum-velocity region was between instrumentation rake locations. When fuel was being burned, however, flashing upstream of the flameholder was observed in the low-velocity region. Average pressure drop across the screen was high, even when the diffuser was operating near the critical point. With a diffuser pressure recovery of 0.634, the pressure ratio across the screen was 0.912 (approximately 9-percent loss).

It is sometimes difficult to determine relative flow distortion by the comparison of flow contours. Therefore, it would be helpful if relative flow distortion could be represented by a generalized parameter. The ratio of the difference between maximum and minimum total pressure to average total pressure is a commonly used parameter for indicating the degree of flow distortion. With the present diffuser, however, the existence of highly localized peak pressures and supersonic flow at the lower values of pressure recovery made this parameter misleading. A parameter that is based on average rather than local values of total pressure, and that includes the static pressure, would therefore be more indicative of flow uniformity and is accordingly used herein. When a supersonic diffuser is operating supercritically at a constant flight Mach number, the relation between Mach number (or the ratio of static to total pressure) at any station in the diffuser and diffuser total-pressure recovery is unique. If flow through the diffuser is greatly distorted, the flow area is not being effectively used; and, for a given average total-pressure recovery, the static pressure at any station would be lower than the static pressure for uniform flow. It was therefore possible to utilize the relation between p_{av}/P_{av} and average total-pressure recovery as a general indication of flow distortion.

Performance of the unmodified diffuser and that of the screen configuration are compared on this basis in figure 10(c). Also included in this figure is a curve showing theoretical variation of the ratio of diffuser-outlet static to total pressure with diffuser pressure recovery for uniform flow. (For derivation of this curve, see appendix B.) Inspection of equation (B4) of appendix B shows that, with a given diffuser-outlet Mach number (or static- to total-pressure ratio), diffuser total-pressure recovery varies inversely with flow area. Therefore, with a given value of static- to total-pressure ratio p_3/P_3, the ratio of theoretical total-pressure recovery to actual total-pressure recovery is equivalent to the ratio of effective to actual diffuser-outlet flow area.

3526

    In general, the trends shown by the Mach number contours are veri-
fied in figure 10(c). With higher values of pressure recovery, the
static pressures obtained with the screen installed are lower than those
obtained with the unmodified diffuser. With a pressure recovery of
about 0.57, the static pressure was slightly higher when the screen was
installed.

    Performance of four-stage vortex-generator configuration (VG-1). -
Although the screen improved flow distribution, combustion upstream of
the flameholder was not completely eliminated and pressure losses were
large. It was apparent that a better method of improving flow distribu-
tion was needed. In the manufacturer's small-scale tests, significant
improvements in flow uniformity were obtained with configurations incor-
porating several stages of vortex generators located a short distance
downstream of the diffuser throat. From the configurations investigated
in the scale model, one that incorporated three stages on the diffuser
innerbody and one stage on the cowl was selected for full-scale evalua-
tion. Positioning of the vortex generators on the innerbody was some-
what unconventional. Instead of placing alternate vanes in a given stage
at opposite angles of attack, all vortex generators on one side of the
duct were at the same angle of attack, while those on the other side were
at the opposite angle of attack (see fig. 5). This arrangement allows
the tip vortices to reinforce each other and results in lateral transla-
tion of the air from the high- to low-velocity regions, in addition to
mixing between the stream and the boundary layer.

    Diffuser-outlet flow contours obtained with configuration VG-1 are
presented in figure 11(a). The contours are, in general, more uniform,
the differences between peak and minimum pressure recoveries are less,
and the peak Mach numbers are lower than obtained with the unmodified
diffuser. The improvement is greatest with intermediate values of pres-
sure recovery (0.594, 0.579, 0.546, and 0.524). Separation, however,
still occurred with pressure recoveries as high as 0.617. Unlike the
original configuration, the size of the separated region was not greatly
increased by reducing pressure recovery below about 0.58. Therefore,
with lower values of recovery (0.546 and 0.501), the separated regions
were smaller than those obtained with the unmodified diffuser.

    The vortex generators also caused a shift in the low-pressure region
from the 2 to the 4 o'clock position. This clockwise shift in flow is
opposite from what might be expected from the angles of attack of the
vortex generators shown in figure 5. With vortex generators, the tip
vortices are used to operate on the flow. Since the portion of the tip
vortices in the high-energy air moves from the high- to the low-pressure
side of the airfoil, its effect on flow translation is opposite to the
effect of guide vanes. This action is illustrated in the following sketch:

—Vortices reeinforce each
other and cause translation
of main stream

—Tip vortices

—Boundary layer
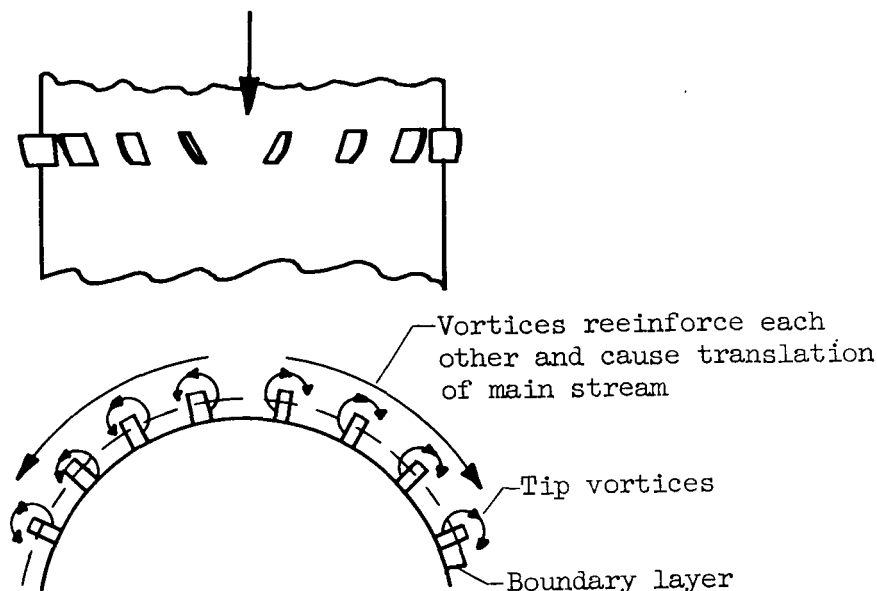
Variation of static- to total-pressure ratio with pressure recovery
for configuration VG-1 is shown in figure 11(b). The curve for the un-
modified diffuser is included for comparison. Significant improvement in
uniformity is indicated at intermediate values of pressure recovery (max-
imum improvement with pressure recovery occurs in range from 0.53 to
0.57). When the diffuser was operating either near the critical point
or at low values of pressure recovery, little improvement is indicated.
These trends are generally in agreement with those shown by the flow
contours. The sharp break in the curve, at a pressure recovery of about
0.54, is probably caused by initiation of supersonic flow in the high-
velocity region.

Performance of 12-stage vortex-generator configuration (VG-2). -
Although four stages of vortex generators gave significant improvement
in flow uniformity, separation still occurred. Additional scale tests
by the manufacturer indicated that further improvement was possible by
the use of more stages. Of many configurations tested in the model, one
incorporating the original three stages on the innerbody, plus five ad-
ditional stages on the innerbody and four stages on the outer duct wall,
appeared to give the best performance and was therefore tested on the
full-scale installation.

Flow contours obtained in the investigation of configuration VG-2
are presented in figure 12(a). For all values of pressure recovery the
difference between maximum and minimum local pressure recovery was less

3526

CA-2

than obtained with any previous configuration. With a pressure recovery of 0.547, the improvement over the four-stage configuration was small. Separation was apparently eliminated with recoveries as low as 0.515 and, in general, minimum Mach numbers were increased and peak Mach numbers reduced.

With pressure recoveries of 0.547 and less, the low-pressure region shifted from the 4 to the 12 o'clock position. Because the low-pressure region occurred at 2 o'clock with the unmodified diffuser, it appeared that the effect of the vortex generators on flow rotation was reversed. With a pressure recovery of 0.547, the diffuser normal shock was near the last stage of vortex generators. Apparently, when flow over the new stages of vortex generators became supersonic, the effect on lateral flow translation diminished. The action of the vortex generators then becomes similar to that of guide vanes.

Variation of the ratio of static to total pressure with pressure recovery is shown in figure 12(b). The curve for the four-stage vortex-generator configuration (VG-1) is included for comparison. The trends shown by the flow contours are generally verified in figure 12(b). Improvement over the previous configuration was indicated with all recovery values, except in the range 0.54 to 0.55. The peaks in the curve at values of pressure recovery of about 0.52, 0.56, and 0.63 are probably caused by the diffuser normal shock passing various stages of vortex generators. Diffuser static-pressure readings showed that all vortex-generator stages were in supersonic flow with recoveries below 0.52 and that all stages were in subsonic flow with recoveries above 0.62.

Effect of vortex-generator span (VG-2). - The full-scale 12-stage vortex-generator configuration had been scaled directly from the manufacturer's 0.15-scale model without Reynolds number corrections. With boundary-layer thickness assumed to vary inversely with Reynolds number to the one-fifth power, a 19-percent reduction of the geometrically scaled vortex-generator spans would be required in order to maintain the same ratio of span to boundary-layer thickness as used in the scale tests. Scale tests also indicated that excessive vortex-generator span could cause unnecessary pressure losses; therefore, it was decided to determine the effect of reducing the spans of the 12-stage configuration by 19 percent. Since the spans of the first three stages of vortex generators (stages A, B, and C) were relatively short, it was assumed that a 19-percent reduction would be insignificant; therefore, these stages were not changed.

Flow contours obtained with the reduced-span configuration (VG-2a) are shown in figure 13(a). With a pressure recovery of 0.616, the contours are about the same as those obtained with longer spans. With a pressure recovery of 0.595, lower values of minimum pressure recovery

and Mach number were obtained with the reduced spans. When pressure recovery was reduced still further $(P_3/P_0 = 0.547)$, flow contours obtained with the reduced-span configuration have slightly smaller spread between maximum and minimum pressure recovery and Mach number.

With configuration VG-2a, the low-velocity region did not shift from the 4 to the 12 o'clock position until pressure recovery was reduced below 0.547, and separation was eliminated with pressure recoveries as low as 0.51. Apparently, reducing the spans helped the vortex generators retain their effectiveness in supersonic flow.

Variation of static- to total-pressure ratio with pressure recovery is shown in figure 13(b). The curves for the longer-span configuration and for the unmodified diffuser are included for comparison. With intermediate values of pressure recovery (0.55 to 0.61), the longer-span configuration gave slightly higher values of static pressure than the short-span configuration. With pressure recoveries above 0.62, the short-span configuration appears slightly better. With recoveries below 0.55, no significant effect of span is visible within the data scatter.

With a pressure recovery of 0.629, the static pressure obtained with the short-span vortex-generator configuration was only slightly higher than that obtained with the unmodified diffuser. The Mach number contours, however, showed that the range of local Mach number variation was from 0.24 to 0.56 with the vortex generators (fig. 13(a)), and from 0.15 to 0.62 with the unmodified diffuser (fig. 9). With a pressure recovery of 0.547, the static- to total-pressure ratio was about 0.79 when the vortex generators were installed and about 0.71 with the unmodified diffuser. With this pressure recovery, the Mach number variation was from 0.19 to 0.80 for the vortex-generator configuration (fig. 13(a)), and large regions of separated and of supersonic flow existed in the unmodified diffuser.

SUMMARY OF RESULTS

An evaluation has been made of several internal modifications incorporated to improve the outlet flow distribution of a side-inlet supersonic diffuser. Among the modifications were a screen (located near the diffuser outlet), a four-stage vortex-generator configuration, and a 12-stage vortex-generator configuration. The effect of reducing the vortex-generator spans of the 12-stage configuration was also determined.

The greatest improvement in flow uniformity was obtained with the 12-stage vortex-generator configuration. The modification with longer spans gave the most uniform distribution when the diffuser was operating at intermediate values of total-pressure recovery (from about 0.55 to

0.61). With pressure recoveries above or below the intermediate range, the reduced-span modification gave the same or slightly better performance. When the unmodified diffuser was operating at a total-pressure recovery of 0.629 (near critical), variations in local Mach number at the diffuser outlet from 0.15 to 0.62 were obtained. With the short-span modification of the 12-stage vortex-generator configuration, the range of variation at this pressure recovery was from 0.24 to 0.56. The diffuser total-pressure recovery at which separation occurred was reduced from about 0.60 with the unmodified diffuser to about 0.51 with the 12-stage vortex-generator configuration with reduced spans.

The four-stage vortex-generator configuration gave considerable improvement in flow uniformity at intermediate pressure recoveries. However, this configuration did not reduce flow separation significantly. Although the screen configuration gave improved flow uniformity, pressure drop across the screen was high (9 percent of screen-inlet total pressure at the critical operation point). Measurements were not taken to determine whether separation was eliminated downstream of the screen. However, 7 inches upstream of the screen, there were, in general, more separation and flow distortions than obtained with the unmodified diffuser.

Lewis Flight Propulsion Laboratory
    National Advisory Committee for Aeronautics
        Cleveland, Ohio, January 4, 1955

APPENDIX A

SYMBOLS

The following symbols are used in this report:

A   cross-section area, sq ft

g   acceleration due to gravity, ft/sec^2

M   Mach number

P   total pressure, lb/sq ft abs

p   average wall static pressure, lb/sq ft abs

R   gas constant, ft-lb/(lb)(^{O}R)

T   total temperature, ^{O}R

t   static temperature, ^{O}R

V   velocity, ft/sec

W   air flow, lb/sec

γ ratio of specific heats

ρ density, lb/cu ft

Subscripts:

av   average

s   free stream

0   supersonic-nozzle inlet

3   diffuser-outlet instrumentation station

3'   instrumentation station behind screen

3526

APPENDIX B

CALCULATIONS

Diffuser total-pressure recovery (P_3/P_0). - Diffuser total-pressure recovery was taken as the ratio of the average total pressure measured at the diffuser-outlet instrumentation station (station 3) to the total pressure measured at the supersonic-nozzle inlet (station 0). The pressure tubes at station 3 were placed at centers of equal area; therefore, area-weighted rather than mass-weighted values of pressure were obtained. Also, any total-pressure losses occurring in the supersonic nozzle are attributed to the diffuser. When the flow was partially supersonic at station 3, no corrections were made for shock losses at the pressure tubes.

Diffuser-outlet Mach number profiles. - Mach numbers were calculated from the ratio of static to total pressure at each of the total-pressure tubes (with $\gamma = 1.38$). Although stream static-pressure tubes were installed, values obtained with these tubes were not reliable. Therefore, the static pressure at each total-pressure tube was determined as follows:

(1) The wall static pressure at each rake was found by plotting wall static pressure against circumferential location of the six wall static taps at station 3.

(2) Static pressure at the center of the duct was assumed to be the average wall static pressure.

(3) Static pressure was assumed to vary linearly along each rake.

Theoretical variation of diffuser-outlet static- to total-pressure ratio p_3/P_3 with diffuser total-pressure recovery P_3/P_0. - The air flow at the diffuser outlet is given by

$$W_3 = \rho_3 A_3 V_3 = \frac{p_3}{Rt_3} A_3 M_3 \sqrt{\gamma g R t_3} = \frac{\sqrt{\frac{\gamma g}{R}} P_3 A_3}{\sqrt{T_3}} \left[\frac{M_3}{\left(1 + \frac{\gamma-1}{2} M_3^2\right)^{\frac{\gamma+1}{2(\gamma-1)}}} \right] \quad (B1)$$

From an air-flow calibration of the engine, the engine air flow was given by

$$W = \frac{0.9607 \, P_0}{\sqrt{T_3}} \quad (B2)$$

Then,

$$\frac{0.9607\ P_0}{\sqrt{T_3}} = \frac{\sqrt{\frac{\gamma g}{R}}\ P_3 A_3}{\sqrt{T_3}} \left[\frac{M_3}{\left(1 + \frac{\gamma - 1}{2} M_3{}^2\right)^{\frac{\gamma + 1}{2(\gamma - 1)}}} \right] \tag{B3}$$

Transposing equation (B3) yields

$$\frac{P_3}{P_0} = \frac{0.9607}{\sqrt{\frac{\gamma g}{R}}\ A_3} \left[\frac{\left(1 + \frac{\gamma - 1}{2} M_3{}^2\right)^{\frac{\gamma + 1}{2(\gamma - 1)}}}{M_3} \right] \tag{B4}$$

where M_3 is determined from

$$\frac{p_3}{P_3} = \left(1 + \frac{\gamma - 1}{2} M_3{}^2\right)^{-\frac{\gamma}{\gamma - 1}} \tag{B5}$$

and

$$\gamma = 1.38$$

$$A_3 = 4.48\ \text{sq ft}$$

The ideal relation between P_3/P_0 and p_3/P_3 was then calculated by using equations (B4) and (B5).

<div align="center">REFERENCE</div>

1. Seashore, Ferris L., and Hurrell, Herbert G.: Starting and Perform-
   ance Characteristics of a Large Asymmetric Supersonic Free-Jet
   Facility. NACA RM E54A19, 1954.

CD-3425

Boundary-layer bleed passage
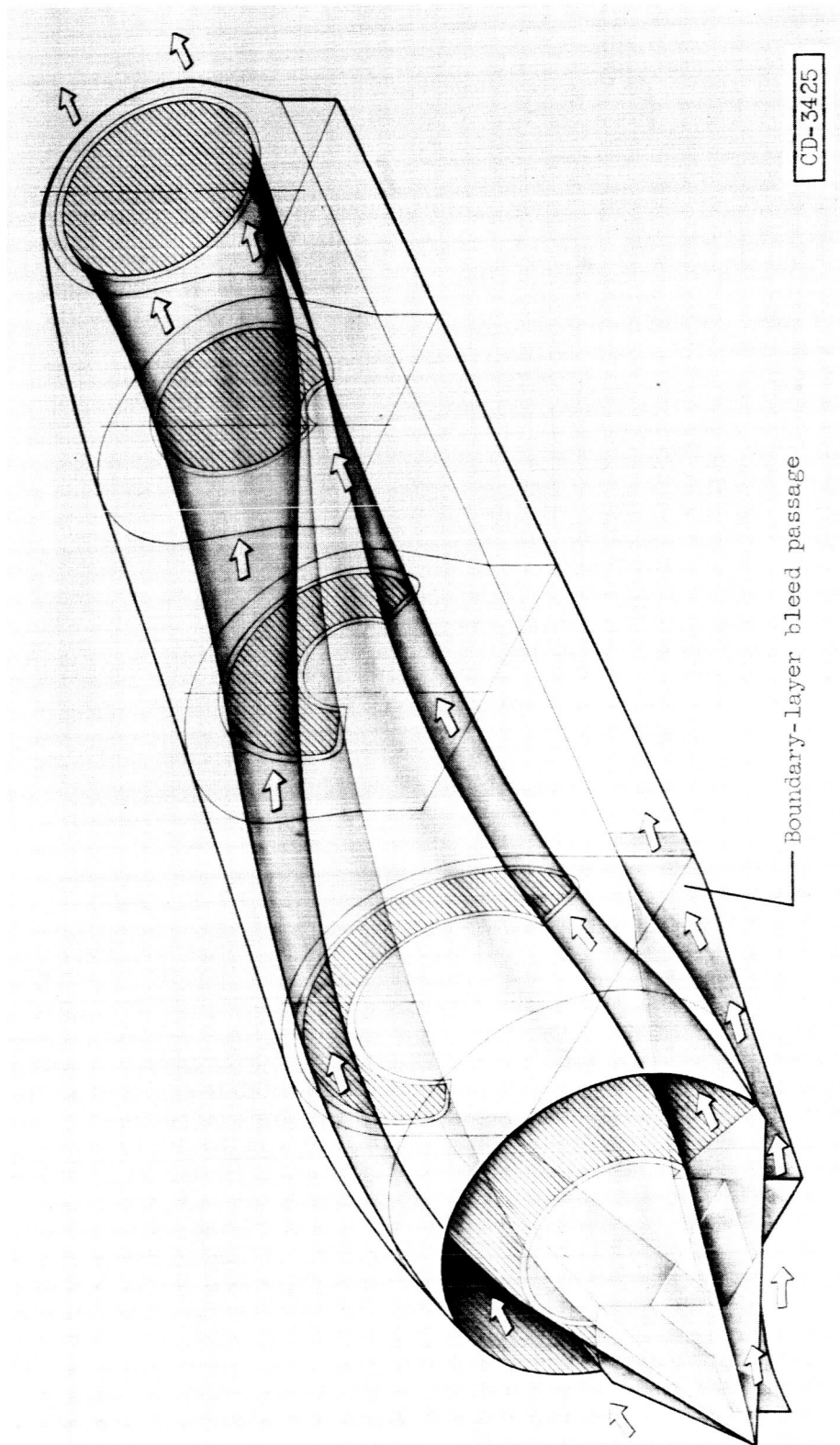
Figure 1. - Phantom view of engine supersonic diffuser.
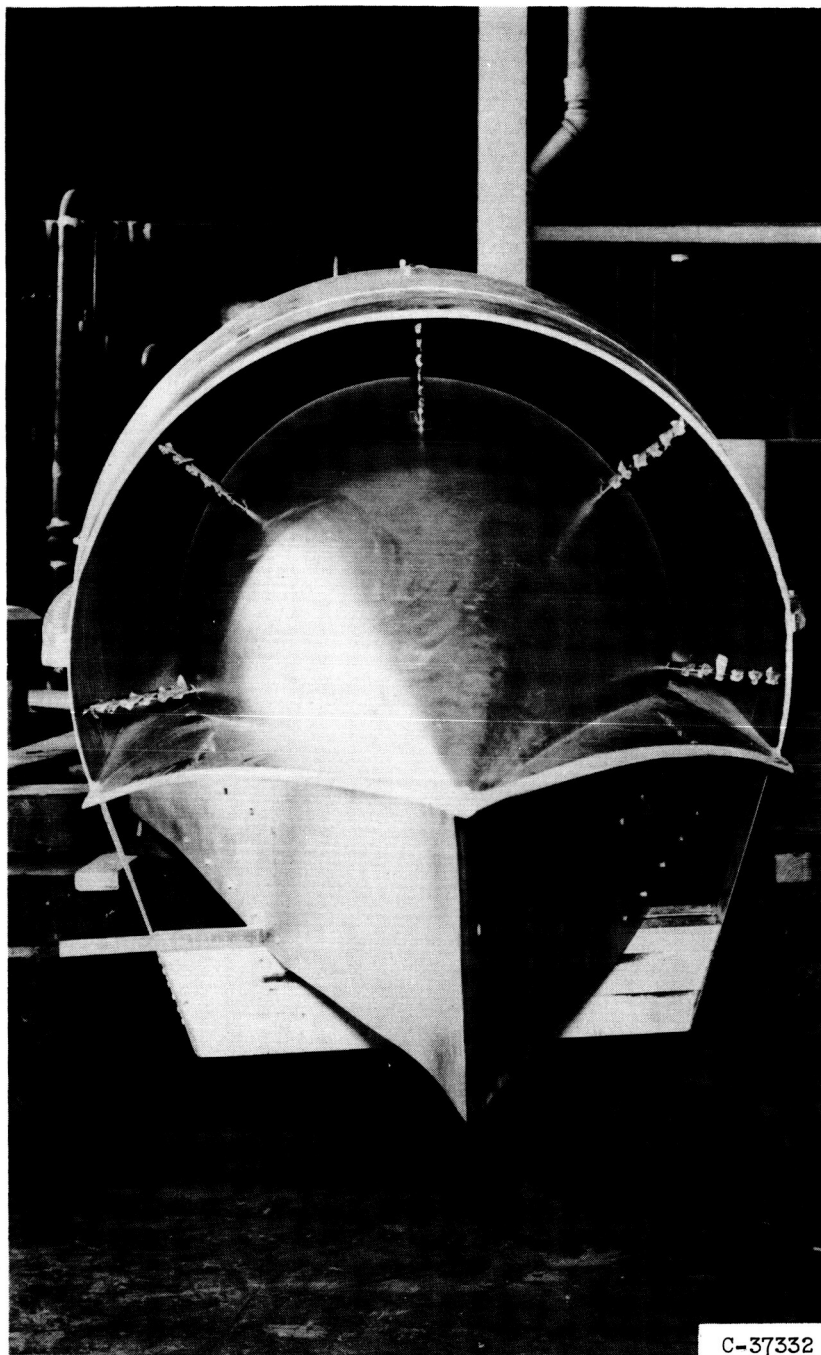
(a) Diffuser inlet.

Figure 2. - Photograph of diffuser.

3526

CA-3
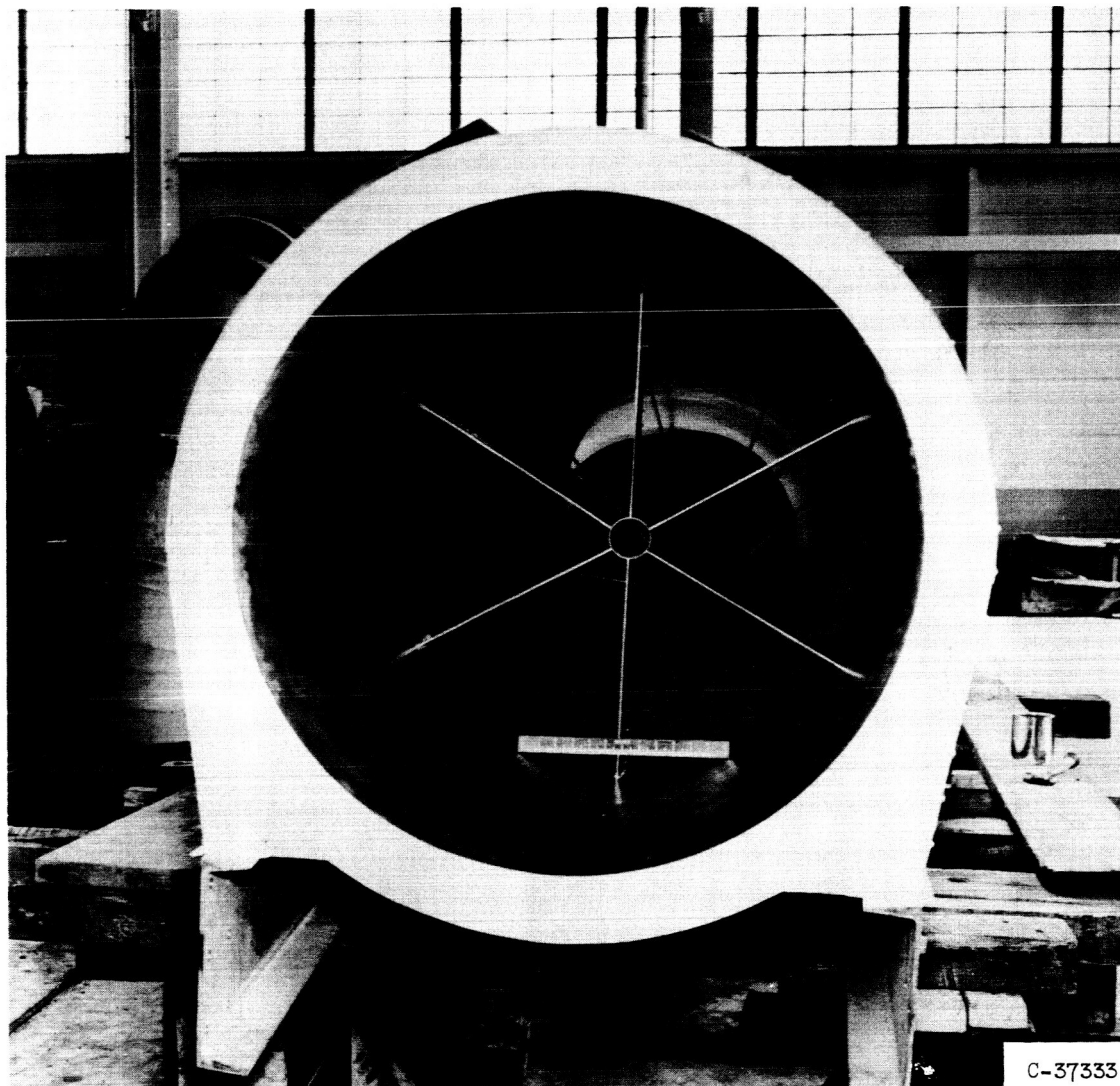
(b) Viewed looking upstream through diffuser duct.

Figure 2. - Concluded. Photograph of diffuser.

3526
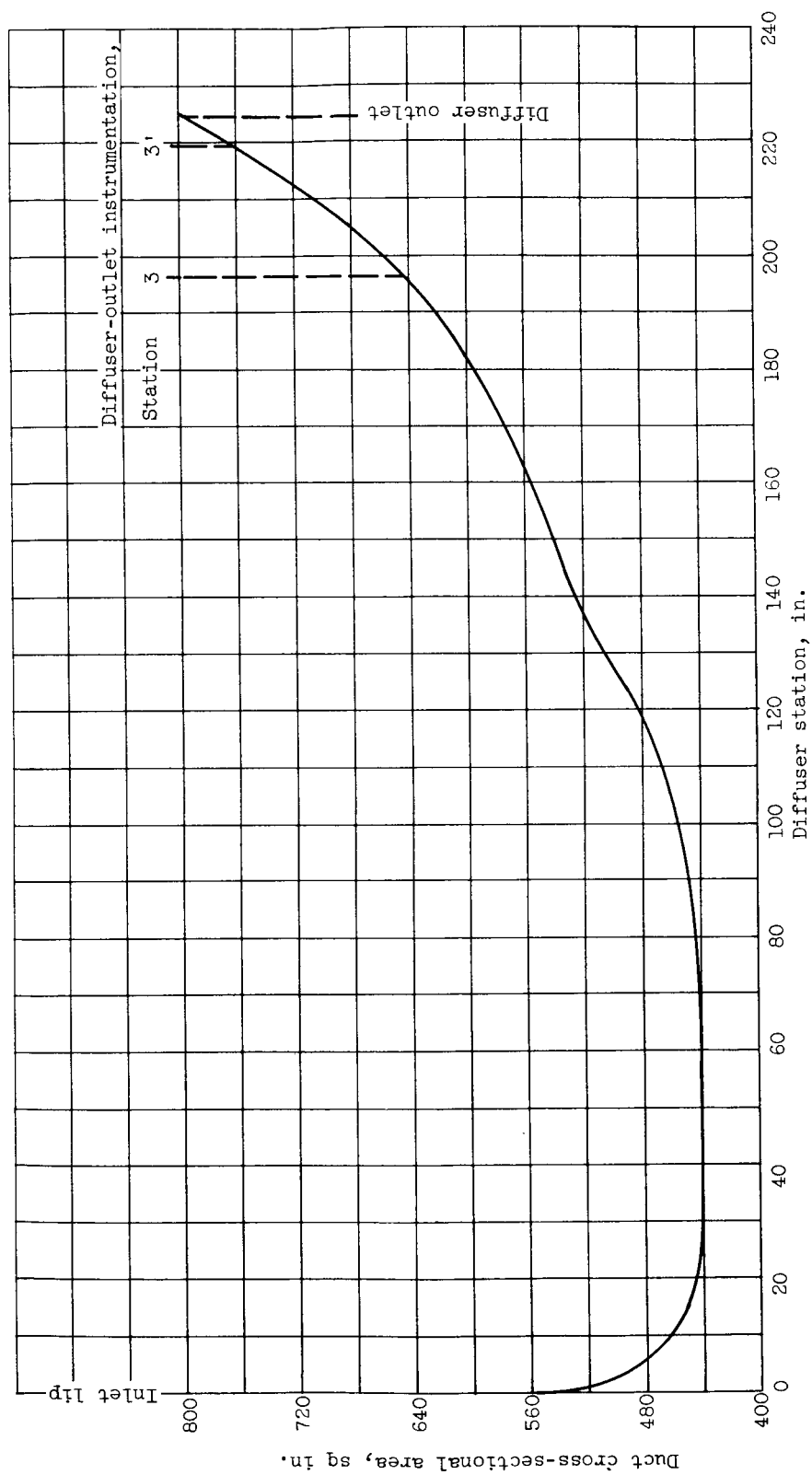
Figure 3. - Area variation through diffuser duct.

3526

CA-3 ,back ,
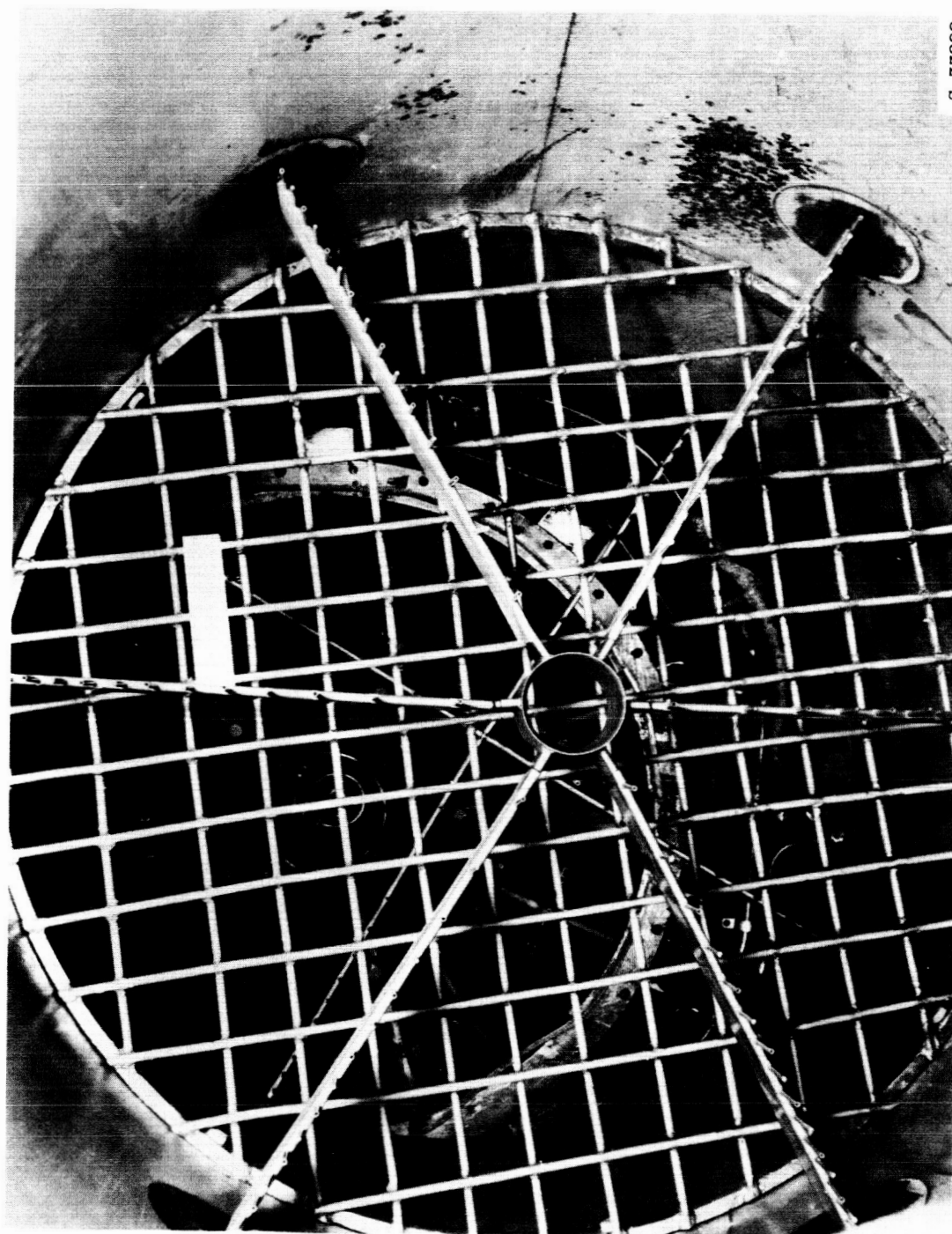
C-33989

Figure 4. - Photograph of installation of screen in diffuser. Viewed looking downstream.

Figure 5. – Description of vortex-generator configurations.
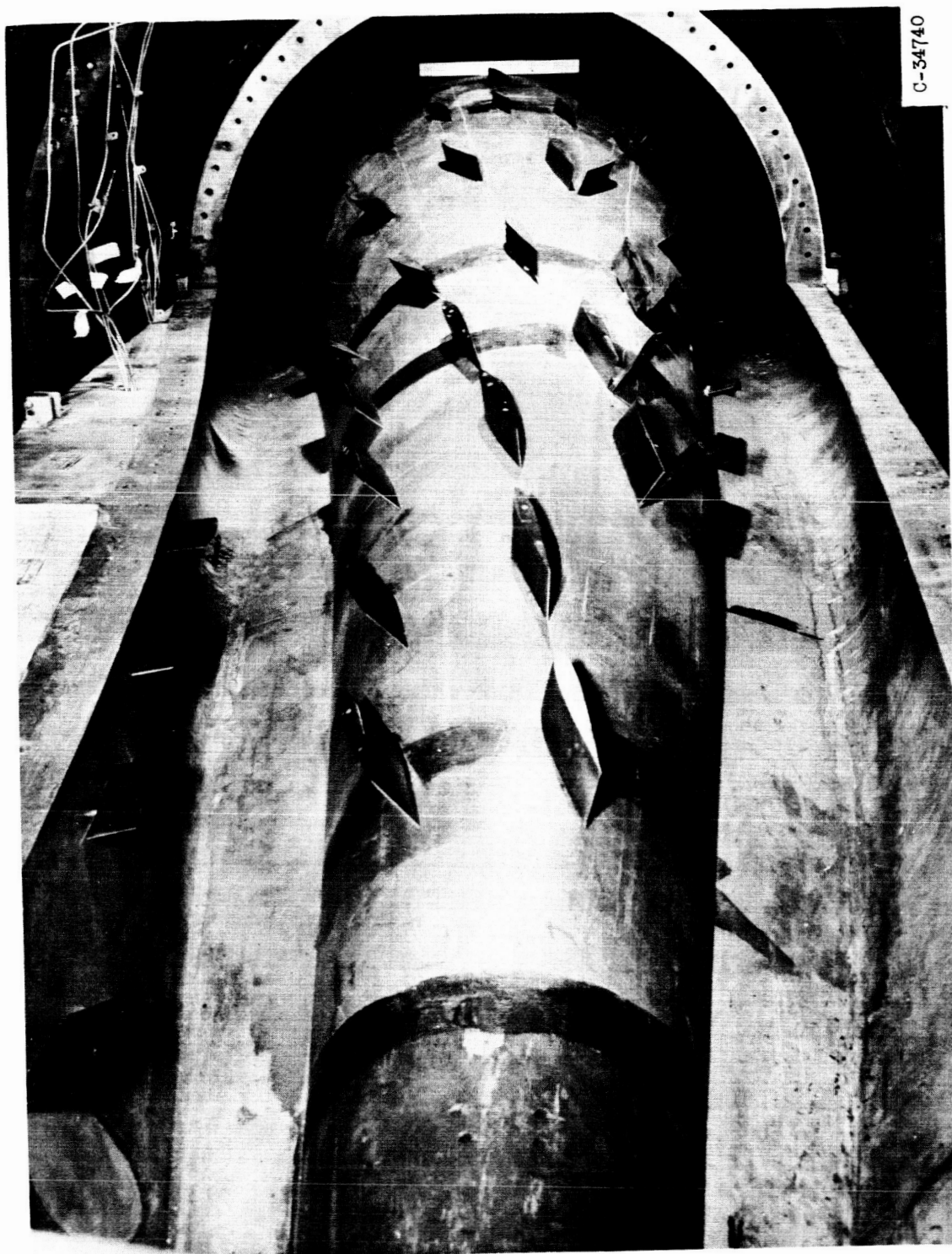
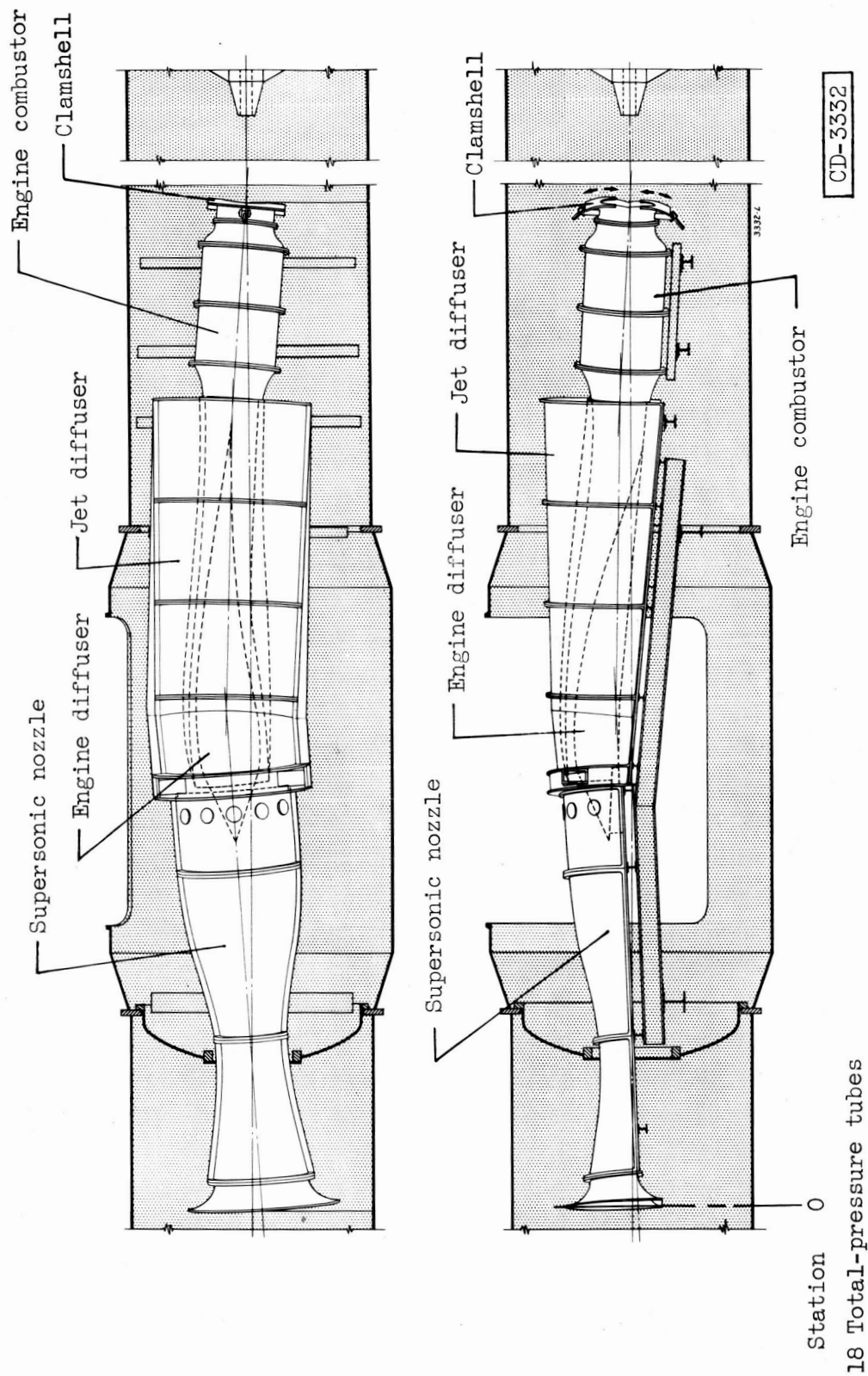Figure 6. - Typical vortex-generator installation. Configuration VG-2. Viewed looking upstream.
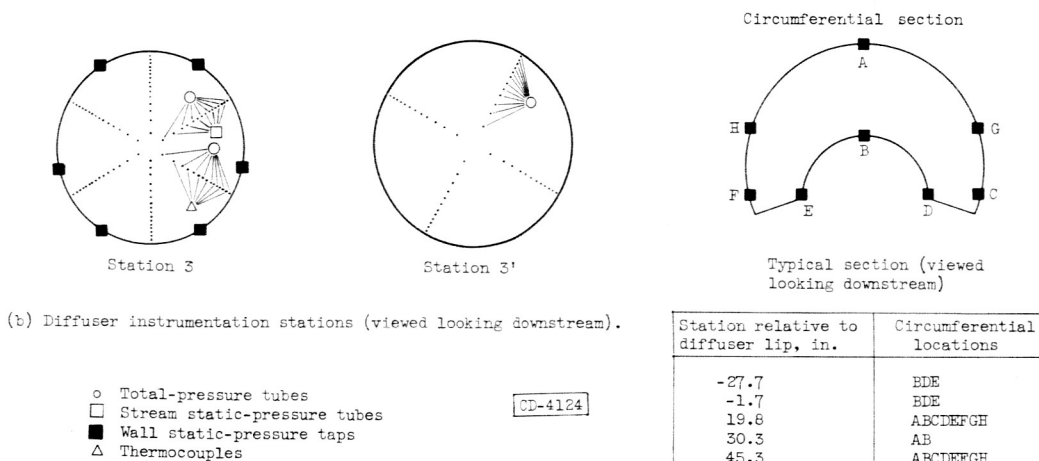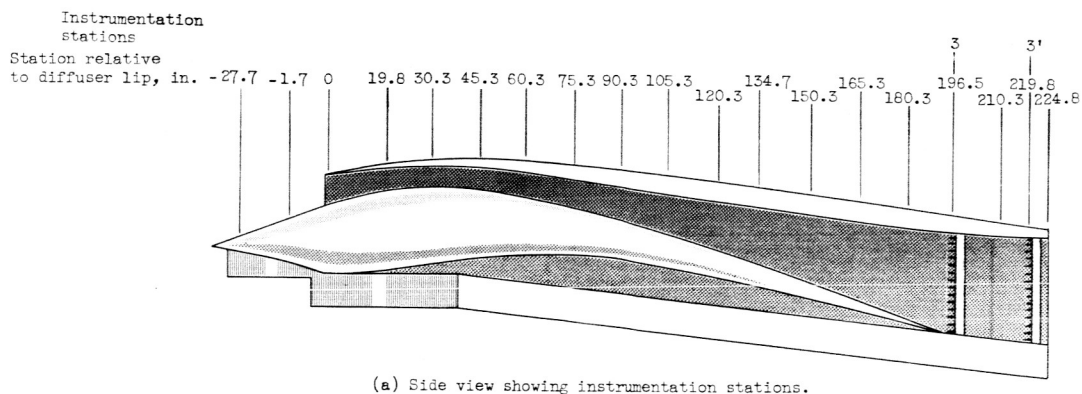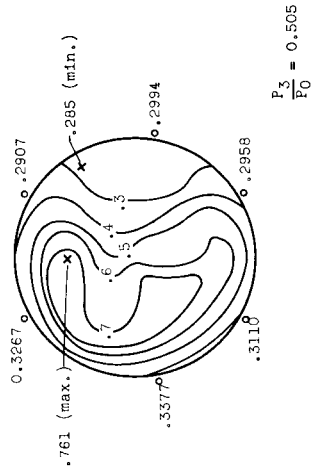
Figure 7. - Free-jet test facility and engine installation

Instrumentation
stations

Station relative
to diffuser lip, in.   -27.7 -1.7 0   19.8 30.3 45.3 60.3 75.3 90.3 105.3   134.7   165.3   196.5   219.8
                                                                            120.3   150.3   180.3   210.3 224.8

(a) Side view showing instrumentation stations.

Circumferential section

Station 3

Station 3'

Typical section (viewed
looking downstream)

(b) Diffuser instrumentation stations (viewed looking downstream).

o Total-pressure tubes
□ Stream static-pressure tubes   CD-4124
■ Wall static-pressure taps
△ Thermocouples

Station relative to diffuser lip, in.	Circumferential locations
-27.7	BDE
-1.7	BDE
19.8	ABCDEFGH
30.3	AB
45.3	ABCDEFGH
60.3	AB
75.3	ABCDEFGH
90.3	AB
105.3	ABCDEFGH
120.3	AB
150.3	AB
165.3	ABCF
180.3	AB
210.3	AB

(c) Location of wall static taps.

Figure 8. - Details of instrumentation.
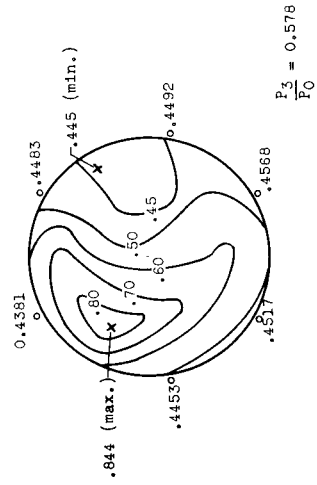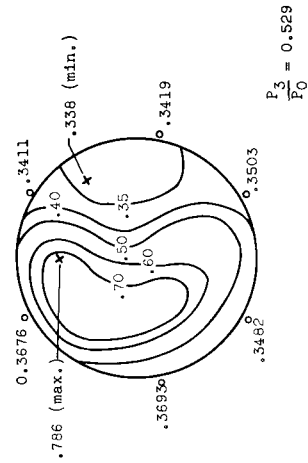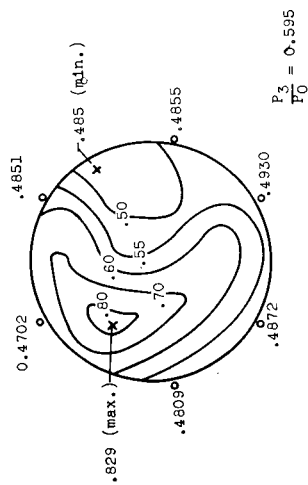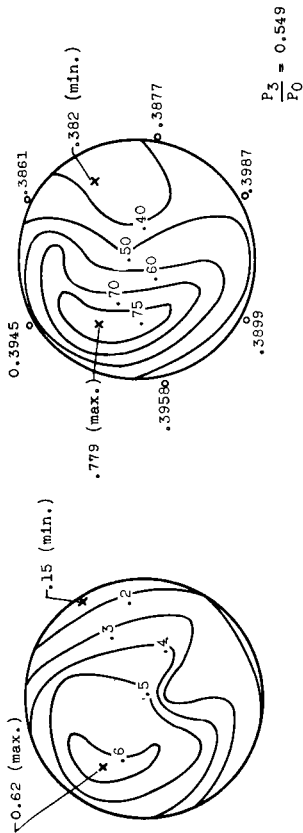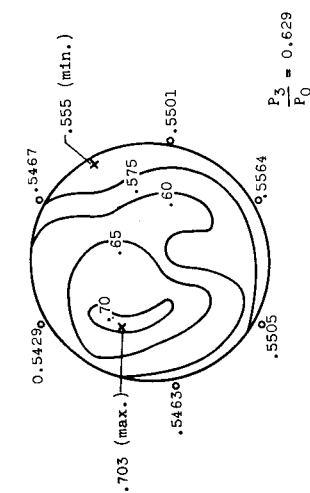
Figure 9. - Diffuser-outlet pressure recovery and Mach number contours obtained with original diffuser configuration. Viewed looking downstream.

○ Wall static pressures, p_3/P_0
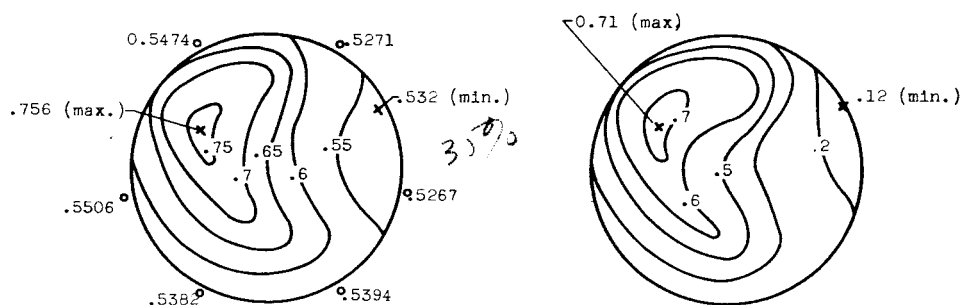
$$\frac{P_3}{P_0} = 0.634$$

$$\frac{P_3}{P_0} = 0.598$$
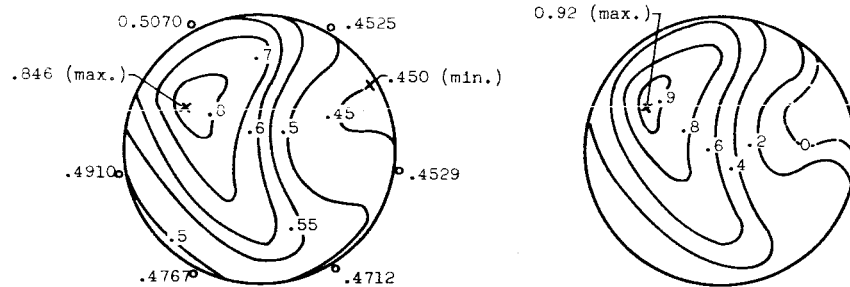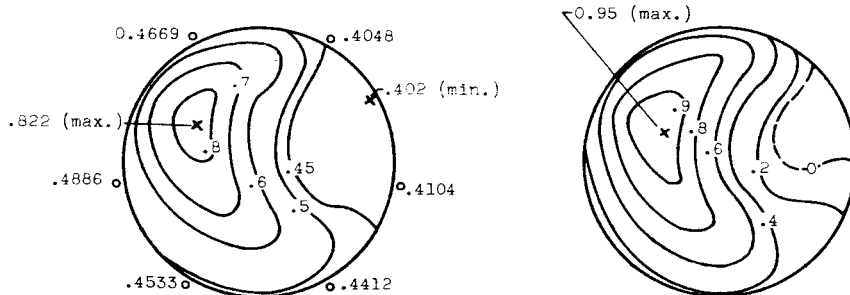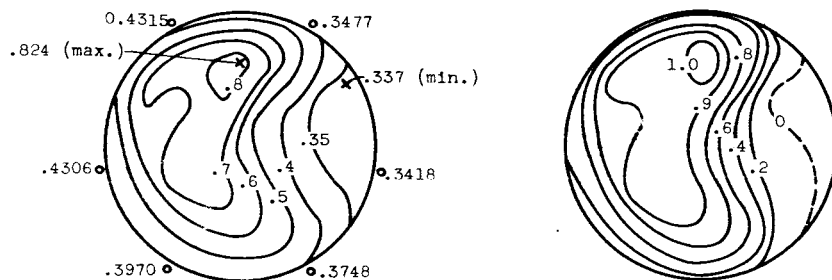
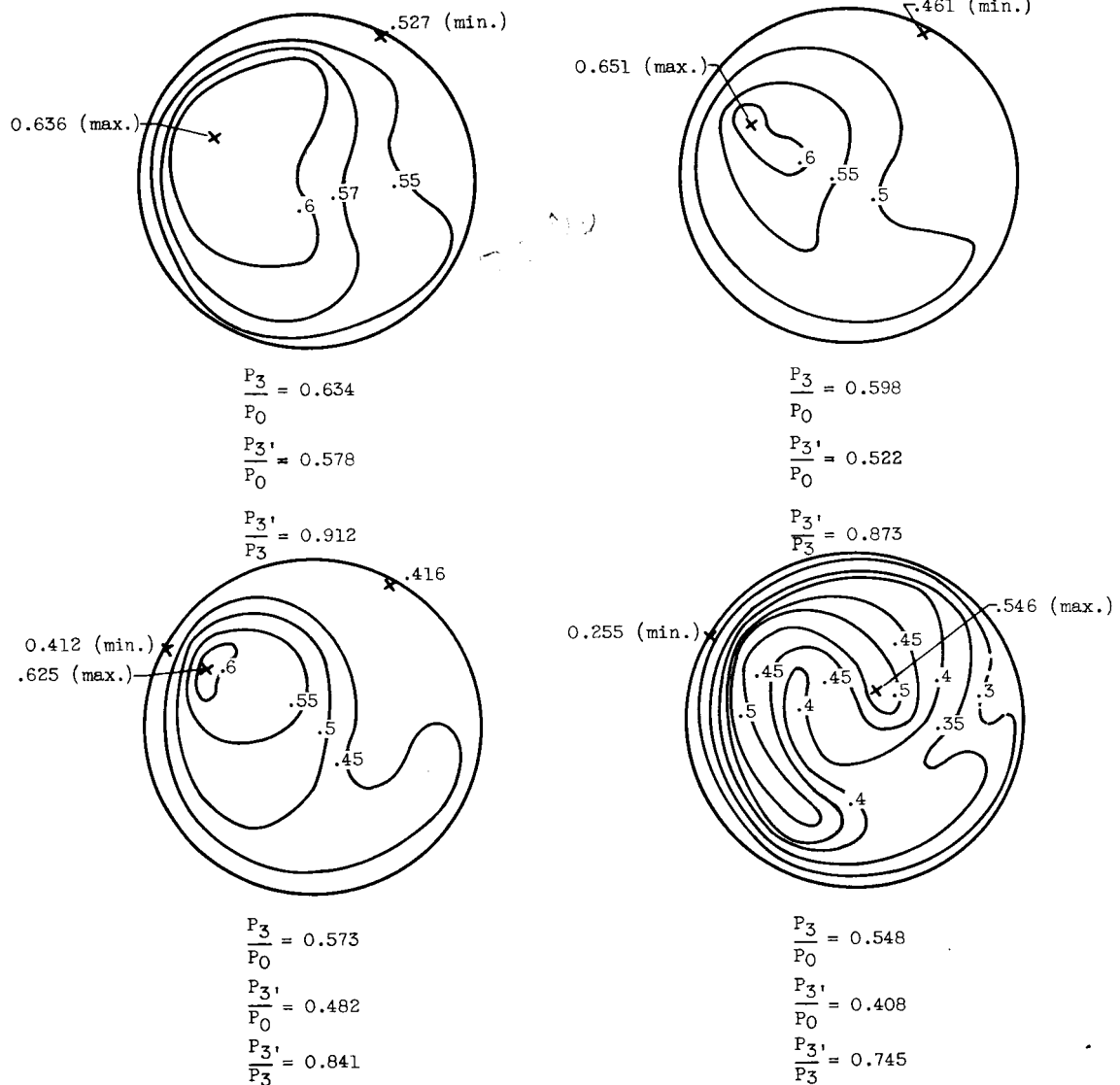$$\frac{P_3}{P_0} = 0.573$$

$$\frac{P_3}{P_0} = 0.548$$

Pressure-recovery contours   Mach number contours
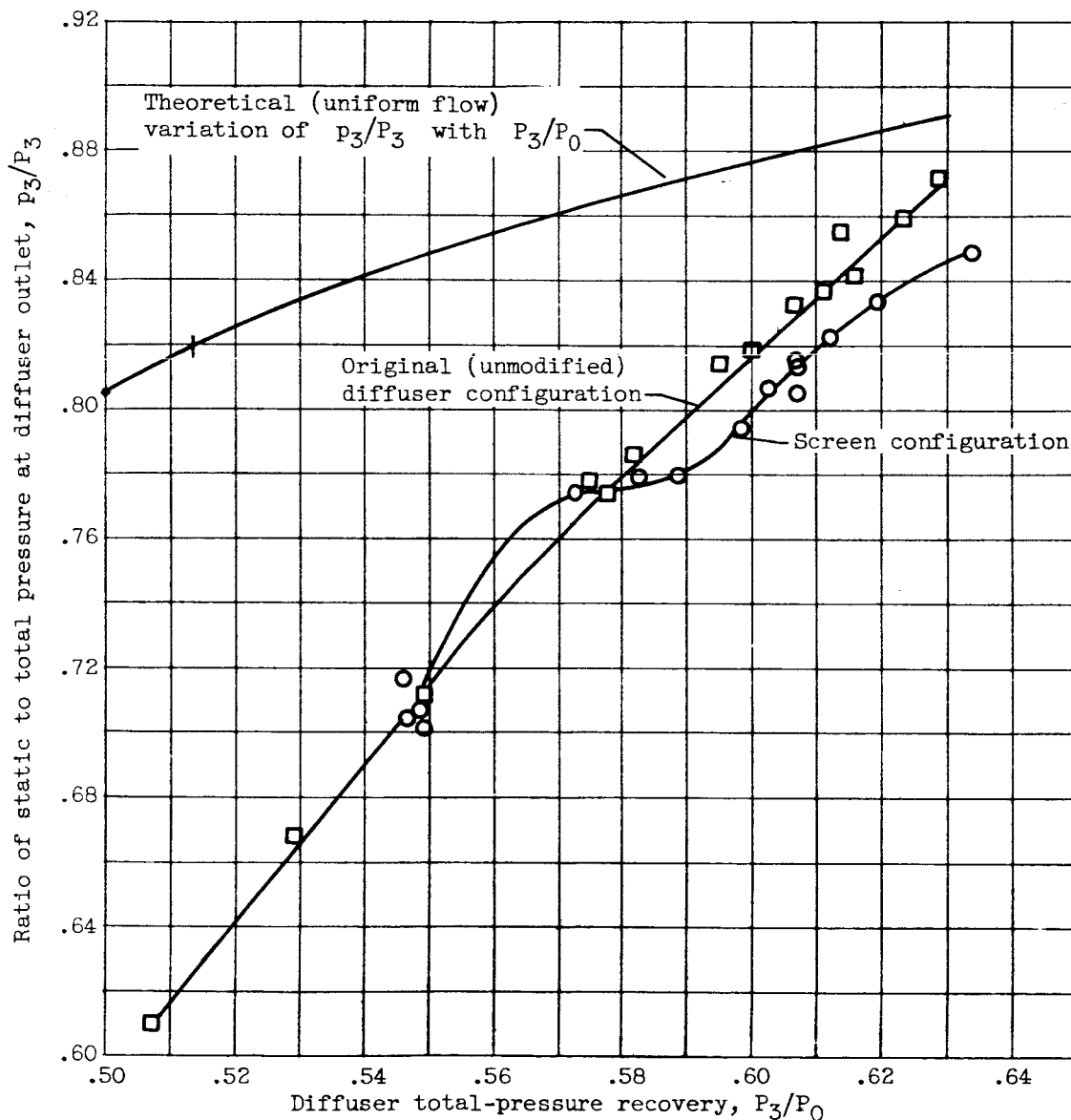
(a) Diffuser-outlet pressure-recovery and Mach number contours (station 3). Viewed looking downstream.

Figure 10. - Performance of screen configuration.

.527 (min.)

.461 (min.)

0.651 (max.)

0.636 (max.)

.57   .55

.6

.6   .55

.5

$\dfrac{P_3}{P_0} = 0.634$

$\dfrac{P_3}{P_0} = 0.598$

$\dfrac{P_3'}{P_0} = 0.578$

$\dfrac{P_3'}{P_0} = 0.522$

$\dfrac{P_3'}{P_3} = 0.912$

$\dfrac{P_3'}{P_3} = 0.873$

.416

.546 (max.)

0.412 (min.)

0.255 (min.)

.625 (max.)   .6

.45

.55   .45   .45   .4

.5   .5   .3

.45

.5   .4   .35

$\dfrac{P_3}{P_0} = 0.573$

.4

$\dfrac{P_3}{P_0} = 0.548$

$\dfrac{P_3'}{P_0} = 0.482$

$\dfrac{P_3'}{P_0} = 0.408$

$\dfrac{P_3'}{P_3} = 0.841$

$\dfrac{P_3'}{P_3} = 0.745$

(b) Pressure-recovery contours behind screen (station 3'). Viewed looking downstream.

Figure 10. - Continued. Performance of screen configuration.

3526

CA-4 back

(c) Variation of diffuser-outlet static- to total-pressure ratio with diffuser total-pressure recovery.

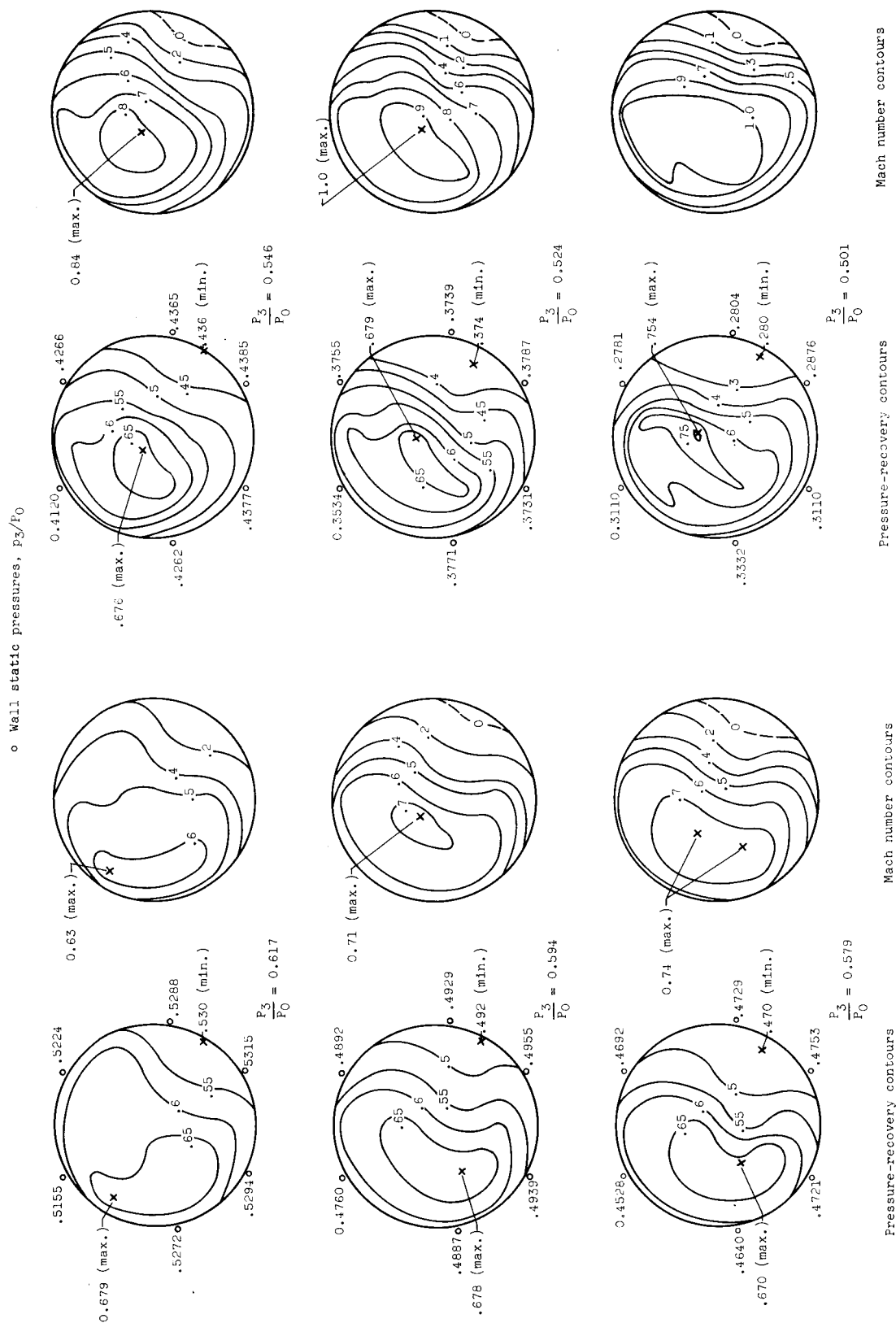Figure 10. - Concluded. Performance of screen configuration.

o Wall static pressures, p_3/P_0

$\frac{P_3}{P_0} = 0.617$

$\frac{P_3}{P_0} = 0.594$

$\frac{P_3}{P_0} = 0.579$

$\frac{P_3}{P_0} = 0.546$

$\frac{P_3}{P_0} = 0.524$

$\frac{P_3}{P_0} = 0.501$

Pressure-recovery contours

Mach number contours

Mach number contours

Pressure-recovery contours

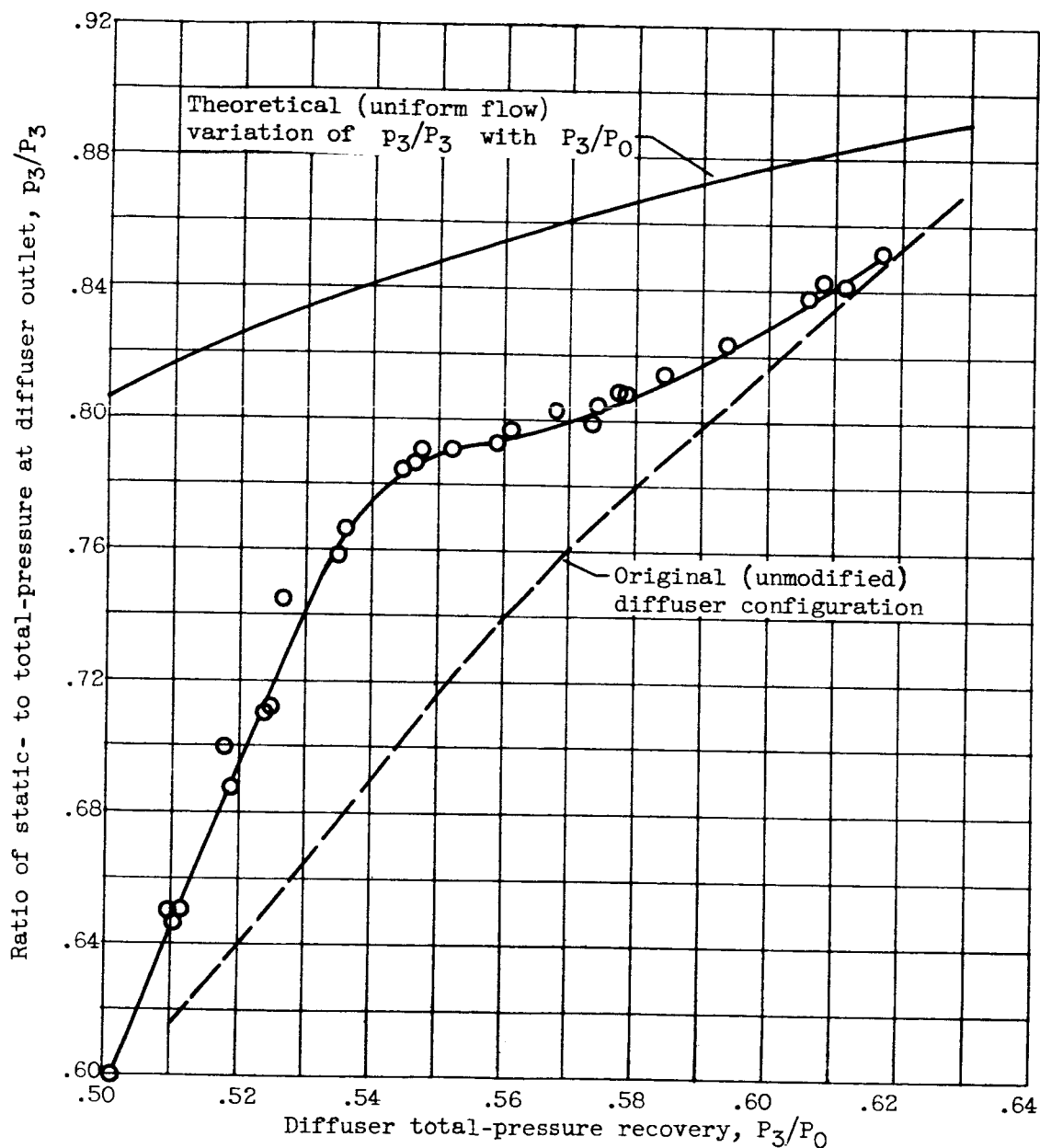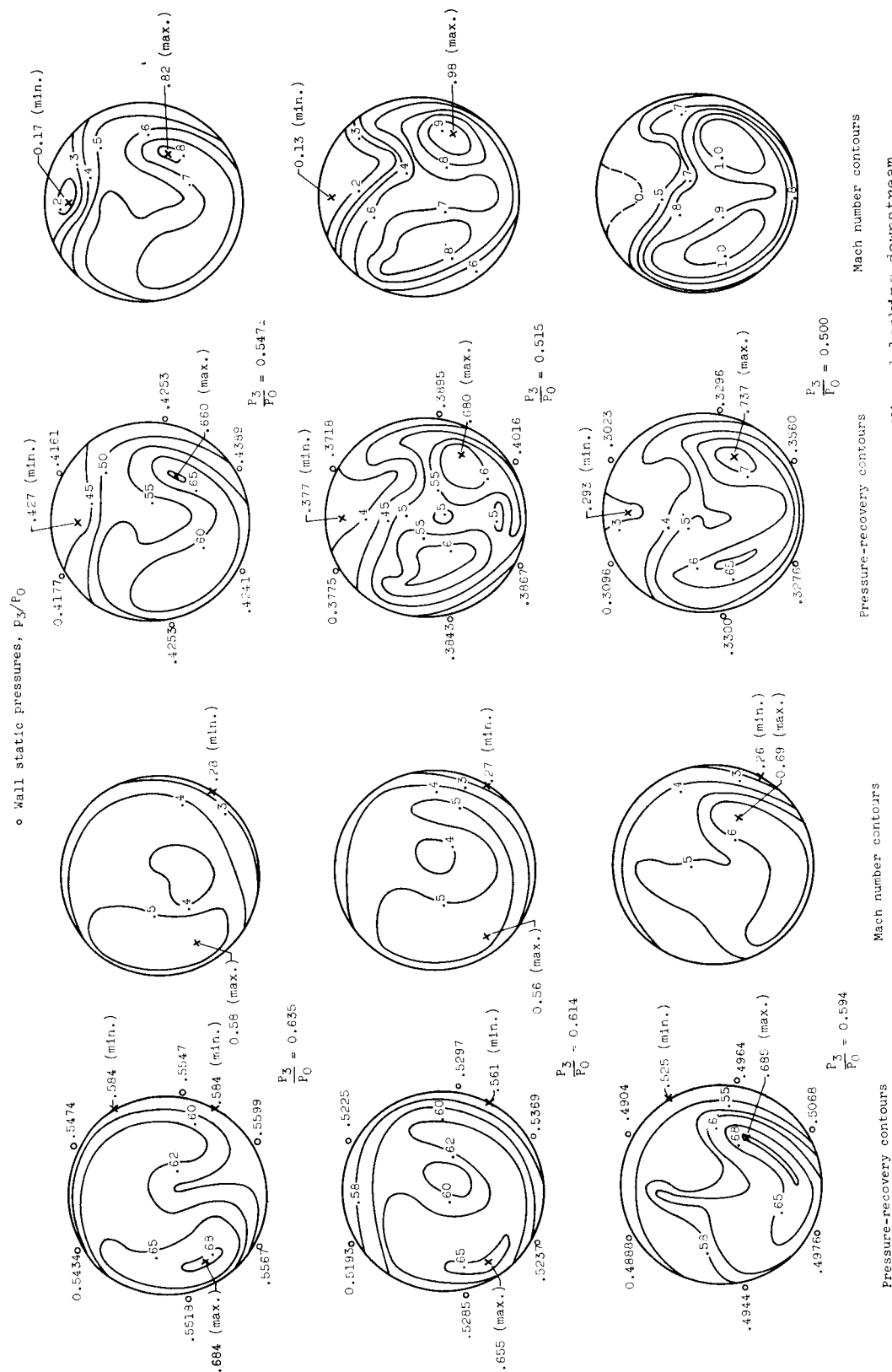(a) Diffuser-outlet pressure recovery and Mach number contours. Viewed looking downstream.

Figure 11. – Performance of four-stage vortex-generator configuration (VG-1).

3526

(b) Variation of diffuser-outlet static- to total-pressure ratio with diffuser total-pressure recovery.

Figure 11. - Concluded. Performance of four-stage vortex-generator configuration (VG-1).

3526

o Wall static pressures, p_3/P_0

$\dfrac{P_3}{P_0} = 0.547$

$\dfrac{P_3}{P_0} = 0.515$

$\dfrac{P_3}{P_0} = 0.500$

Pressure-recovery contours

Mach number contours

(a) Diffuser-outlet pressure recovery and Mach number contours. Viewed looking downstream.

$\dfrac{P_3}{P_0} = 0.635$

$\dfrac{P_3}{P_0} = 0.614$

$\dfrac{P_3}{P_0} = 0.594$

Mach number contours

Pressure-recovery contours

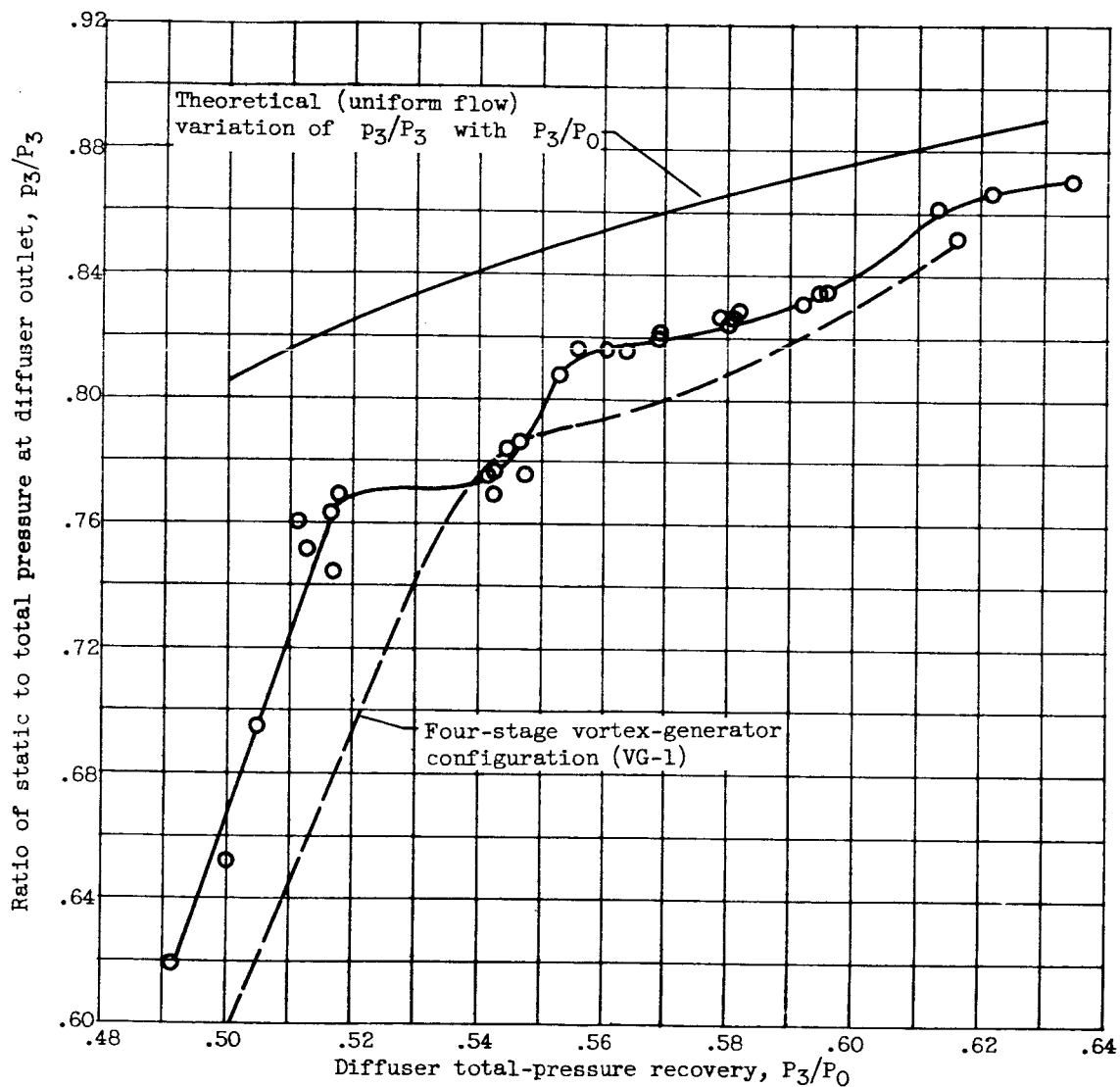Figure 12. - Performance of 12-stage vortex-generator configuration (VG-2).

3526

(b) Variation of diffuser-outlet static- to total-pressure ratio with diffuser total-pressure recovery.

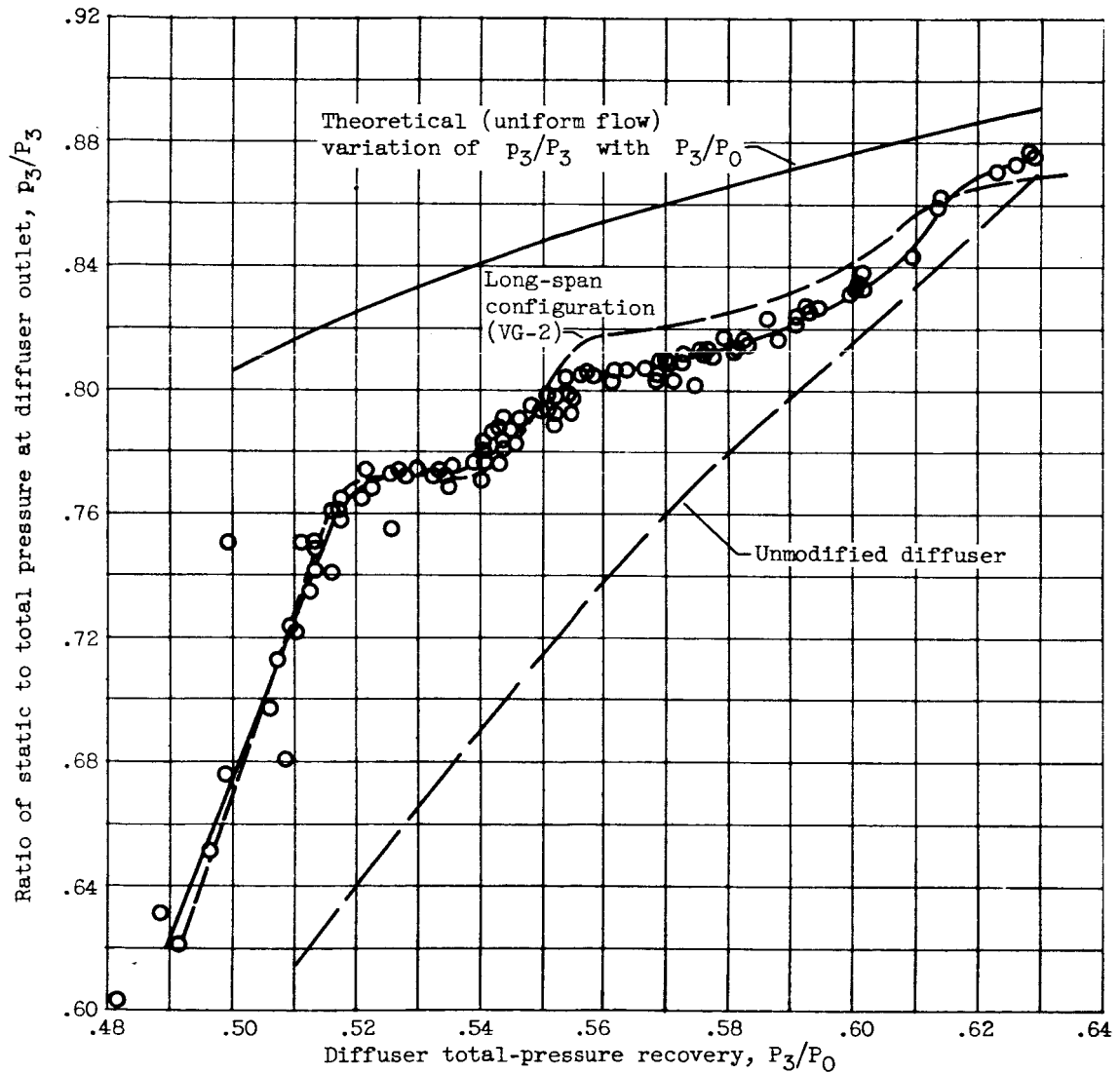Figure 12. - Concluded. Performance of 12-stage vortex-generator configuration (VG-2).

o Wall static pressures, p_3/P_0

Pressure-recovery contours

Mach number contours

(a) Diffuser-outlet pressure-recovery and Mach number contours. Viewed looking downstream.

Figure 13. - Performance of 12-stage vortex-generator configuration with reduced spans (VG-2a).

3526

(b) Variation of diffuser-outlet static- to total-pressure ratio with diffuser total-pressure recovery.

Figure 13. - Concluded. Performance of 12-stage vortex-generator configuration with reduced spans (VG-2a).